PHYSICAL REVIEW E **72**, 025201(R) (2005)

Basins of attraction in piecewise smooth Hamiltonian systems

Ying-Cheng Lai,[1] Da-Ren He,[2,3] and Yu-Mei Jiang[3]
[1]*Department of Electrical Engineering, Arizona State University, Tempe, Arizona 85287, USA*
[2]*CCAST (World Laboratory), P. O. Box 8730, Beijing, China 100080*
[3]*College of Physics Science and Technology, Yangzhou University, Yangzhou, China 225002*
(Received 24 March 2005; published 1 August 2005)

Piecewise smooth Hamiltonian systems arise in physical and engineering applications. For such a system typically an infinite number of quasiperiodic "attractors" coexist. (Here we use the term "attractors" to indicate invariant sets to which typically initial conditions approach, as a result of the piecewise smoothness of the underlying system. These "attractors" are therefore characteristically different from the attractors in dissipative dynamical systems.) We find that the basins of attraction of different "attractors" exhibit a riddledlike feature in that they mix with each other on arbitrarily fine scales. This practically prevents prediction of "attractors" from specific initial conditions and parameters. The mechanism leading to the complicated basin structure is found to be characteristically different from those reported previously for similar basin structure in smooth dynamical systems. We demonstrate the phenomenon using a class of electronic relaxation oscillators with voltage protection and provide a theoretical explanation.

DOI: 10.1103/PhysRevE.72.025201 PACS number(s): 05.45.−a

A fundamental goal in science is to make predictions. For systems that evolve in time, a basic question is: for a given initial condition where does the trajectory go? Often, there are multiple coexisting destinations, e.g., attractors in dissipative systems, each having its own basin of attraction. For an initial condition near a basin boundary, uncertainty in the prediction of the final attractor can arise because of the finite precision in the specification of the initial condition. In order to improve the predictability, a possible way is to make the initial condition more precise. If the basin boundary is simple, e.g., a one-dimensional curve in a two-dimensional phase space, increasing the precision will result in an equal amount of improvement in the predictability of the attractor. It has been recognized, however, that in nonlinear dynamical systems significant difficulty can arise in the prediction of the final destination. In particular, fractal basin boundaries [1–3] can arise for which improvement in the precision to specify the initial condition often results in disproportionally less improvement in the predictability. Dynamical systems, especially those possessing a simple symmetry, can have riddled basins [4,5], for which vast increase in the precision of the initial condition results in practically no improvement in the predictability. The predictability is usually characterized by examining how the probability of error in the prediction, $f(\epsilon)$, scales with the precision ϵ in the initial condition. One typically has $f(\epsilon) \sim \epsilon^{\alpha}$, where $0 \leqslant \alpha \leqslant 1$ is the uncertainty exponent [1]. The value of α determines the degree of improvement in the predictability [i.e., decrease in $f(\epsilon)$] upon reduction in ϵ. For fractal basin boundaries, the typical values of α are between zero and unity, while for riddled basins, $\alpha \approx 0$.

Situations where the uncertainty exponent α assumes near-zero value are of concern because it implies an extreme type of unpredictability of the system's destinations. The mechanism underlying this property seems to be well understood in the case of riddled basins [4–6]. That riddling typically occurs in dynamical systems with a symmetry does not mean that systems without symmetry are immune to the extreme type of unpredictability. Because of the fundamental importance of predictability in science, it is of broad interest to identify dynamical mechanisms other than riddling that can cause a similar degree of unpredictability.

In this paper, we present a class of nonsymmetrical physical systems that exhibit such an extreme degree of unpredictability of attractors. The system is piecewise smooth Hamiltonian with a bifurcation parameter p that controls the degree of nonsmoothness. Say for $p=p_c=1$ the system is smooth and described by a Hamiltonian map in the entire phase-space region of interest, which typically contains Kol'mogorov-Arnol'd-Moser (KAM) islands and chaotic sea. Imagine that for $p<p_c$ a subregion in the phase space emerges in which the dynamics is governed by a different smooth Hamiltonian map. The system then becomes piecewise smooth for $p<p_c$, with two distinct phase-space regions (denoted by Σ_1 and Σ_2) in which the maps are different but are still Hamiltonian by themselves. Invariant sets located entirely in each region, typically KAM tori, remain to be invariant. However, the original chaotic sea may now locate in both Σ_1 and Σ_2 and so it is no longer invariant. As a result, trajectories initiated in the original chaotic sea will become *transiently* chaotic and eventually approach one of the KAM tori, making them effectively attracting sets. There can then be an infinite number of such "attractors" in the phase space for $p \lesssim p_c$. Due to the appearence of "attractors," the system becomes effectively dissipative ("quasidissipative" [7]) but the final "attractors" are tori that generate various quasiperiodic motions. We find that the basins of attraction arising in such quasidissipative systems are mixed in such a way that for every initial condition that approaches one "attractor," there are initial conditions arbitrarily nearby that approach other "attractors," making $\alpha \approx 0$. The mechanism for the occurrence of a near-zero uncertainty exponent is found to be different from riddling. As we will show, it is due to the *mixing of different basins of attraction on a fat-fractal set*. The situation can be expected to occur in physical

systems, as we shall demonstrate using a class of electronic oscillators that find applications in physical and engineering devices.

We consider a class of electronic relaxation oscillators with voltage protection [8]. The circuit consists of a capacitor connected in parallel with two constant current sources, each controlled by an electronic switch. The capacitor can be charged or discharged in different time intervals. In the absence of voltage protection, the switches provide an upper voltage threshold that varies sinusoidally with time: $U_1(t)=U_{max}-U_0\sin(\omega t)$, and a lower threshold $U_2(t)$, where U_{max}, U_0, and ω are parameters, and $U_2(t)$ is a function of time. Between the thresholds, the voltage $V(t)$ across the capacitor varies linearly with time. Say at time t_n, $V(t)$ reaches the upper threshold: $V(t_n)=U_1(t_n)$. For $t>t_n$, $V(t)$ decreases until it reaches $U_2(t)$ at some time $t^*>t_n$, and starts to arise for $t>t^*$, and reaches $U_1(t)$ at t_{n+1}, and so on. Let x_n denote the phase of $U_1(t)$. An elementary circuit analysis leads to a one-dimensional discrete-time map relating x_{n+1} to x_n [9]. Voltage protection is introduced by setting the upper threshold to a constant E in the time intervals during which $V(t)>E$. The region in the phase variable x where voltage protection is in effect is then $F=[x_{F_1},x_{F_2}]=[1/2+\sin^{-1}c/(2\pi),1-\sin^{-1}c/(2\pi)]$, where $c\equiv E/U_0$. Similarly, a new phase variable y_n can be used to model the dynamics at the lower threshold and it can be assumed that $U_2(t)$ depends linearly on y_n [8]. The charging and discharging process of the capacitor can then be described by a two-dimensional map in terms of the phase variables (x_n,y_n). Because of the voltage-protection mechanism, the map takes a different form outside and inside the region F. Since the dynamics is governed by phase variables, both maps are area preserving. The system is thus described by piecewise smooth Hamiltonian maps [8], as follows: for $x_n\notin F$,

$$x_{n+1}=\left[x_n+y_{n+1}+\frac{a}{b}\right]\mathrm{mod}(1),$$

$$y_{n+1}=\left[y_n-\frac{\sin(2\pi x_n)}{b}\right]\mathrm{mod}(1), \qquad (1)$$

but for $x_n\in F$,

$$x_{n+1}=\left[x_n+y_n+\frac{a+c}{b}\right]\mathrm{mod}(1),$$

$$y_{n+1}=[y_n+2x_n]\mathrm{mod}(1), \qquad (2)$$

where a and b are parameters. Note that for $c=1$, the voltage-protection region F vanishes, leaving a smooth Hamiltonian map given by Eq. (1) only. The phase-space structure in this case is well understood [10], which typically contains KAM tori and chaotic seas, as shown in Fig. 1(a) for $a=2.0$ and $b=4.0$. As c is decreased from unity, the system becomes piecewise smooth as modeled by both Eqs. (1) and (2). Our interest here is in the slightly nonsmooth region: $c\lesssim 1$.

For $c\lesssim 1$, the voltage-protection region F appears. As a result, a set originally invariant under map Eq. (1) for $c=1$ will cease to be so, if it overlaps with F. Since the large chaotic sea around the center of Fig. 1(a) extends to a substantial region of the phase space, the region F, as soon as it appears, passes through the sea. As a result, the chaotic sea is no longer invariant, leading to *transient chaos*. Trajectories originated from initial conditions in the chaotic sea will leave it in finite time. In fact, a nonattracting chaotic set (chaotic saddle) arises as soon as c is decreased from unity. In the meantime, invariant sets that do not overlap with F, typically KAM islands, remain invariant. Because of the transient nature of chaotic trajectories, they eventually approach one of the KAM islands. In this sense, the islands can be regarded effectively as "attractors." An example of such "attractors" is shown in Fig. 1(b) for $c=0.999$, where the two vertical parallel lines indicate the voltage-protection region F and the "attractors" are generated by using a uniform grid of 10×10 initial conditions in the square box $[0.4\leqslant(x,y)\leqslant 0.6]$ at the center of Fig. 1(a). Because of the appearance of "attractors," piecewise smooth Hamiltonian systems resemble dissipative systems, hence the terminology "quasidissipative" dynamical systems [8]. Because of the hierarchical structure of KAM islands in the smooth system for $c=1$, there can in principle be an infinite number of "attractors" for $c\lesssim 1$.

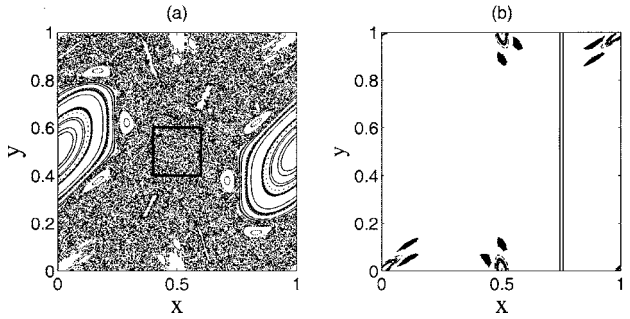

FIG. 1. (a) Phase-space structure of the smooth Hamiltonian map Eq. (1) for $c=1$. Shown are KAM islands and chaotic sea for $a=2.0$ and $b=4.0$ obtained from a uniform grid of 10×10 initial conditions in the unit square. (b) For $c=0.999$, the original chaotic motion becomes transient and KAM islands located either completely outside F or completely inside F become "attractors."

To compute the basins of attraction, we use the fact that the "attractors" are quasiperiodic and so, it is convenient to use the winding numbers to numerically distinguish them. For a trajectory $\{x_n,y_n\}_{n=1}^N$, the winding numbers are $W_x=\lim_{N\to\infty}(1/N)\Sigma_{n=1}^N|x_{n+1}-x_n|$ and $W_y=\lim_{N\to\infty}(1/N)\Sigma_{n=1}^N|y_{n+1}-y_n|$. Figures 2(a) and 2(b) show, for $c=0.999$, the distributions of winding number W_x and W_y, respectively, from a uniform grid of 100×100 initial conditions in the central box in Fig. 1(a), where for each initial condition, the number of iterations used is $N=2\times 10^5$. There are several localized regions for the winding numbers. For convenience, we (arbitrarily) choose $\bar{W}_y=0.55$ as the threshold for distinguishing two clusters of "attractors:" one for $W_y<\bar{W}_y$ (cluster I) and another for $W_y>\bar{W}_y$ (cluster II), as shown in Fig. 2(b). We then use a denser grid of 500×500 initial conditions from the same box and determine for each initial condition whether the resulting "attractor" belongs to

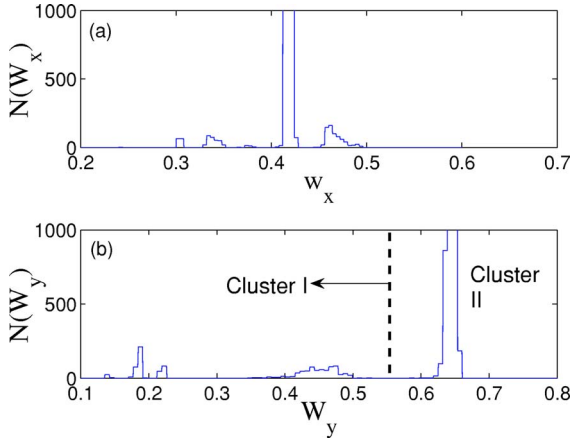

FIG. 2. (Color online) For $c=0.999$, distributions of winding numbers W_x (a) and W_y (b).

cluster I or II according to its winding number W_y. Figure 3(a) shows, in black dots, the initial conditions that generate "attractors" in cluster I, i.e., the basin of the cluster-I "attractors," while blank regions denote the basin of the cluster-II "attractors." The two basins are apparently mixed in a random manner and the pattern persists when smaller and smaller scales are examined, indicating a riddledlike structure that practically prevents prediction of "attractors" from a given initial condition. Figure 3(b) shows the fraction $f(\epsilon)$ of uncertain initial conditions leading to trajectories that go to different clusters upon perturbation ϵ, which was obtained by randomly choosing initial-condition pairs (x_0,y_0) and $(x_0+\epsilon/\sqrt{2},y_0+\epsilon/\sqrt{2})$ in the square box $0.4\leqslant(x,y)\leqslant0.6$, varying the number of pairs, and accumulating 1000 uncertain initial-condition pairs. We see that over seven orders of magnitude of variation in ϵ do not apparently reduce $f(\epsilon)$, i.e., $\alpha\approx0$, indicating the extreme type of unpredictability of "attractors" that is characteristic of riddled basins [4]. Numerically, we find that the riddled features are independent of the choice of the clusters. For instance, by using a different value of the winding number for classifying "attractors," basin structures similar to those in Fig. 3 were observed.

We now explain the riddledlike structure in general piecewise smooth Hamiltonian systems. For concreteness we consider a system with phase space divided into two distinct but

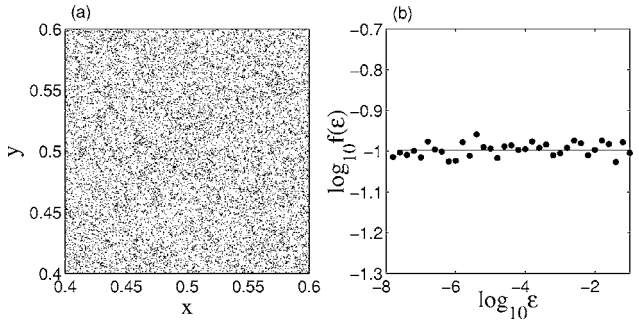

FIG. 3. For $c=0.999$, (a) basin of attraction of "attractors" in cluster I (black dots) as defined in Fig. 2(b) and, (b) fraction $f(\epsilon)$ of uncertain initial-condition pairs vs the perturbation strength ϵ. The estimated uncertainty exponent is $\alpha\approx0$.

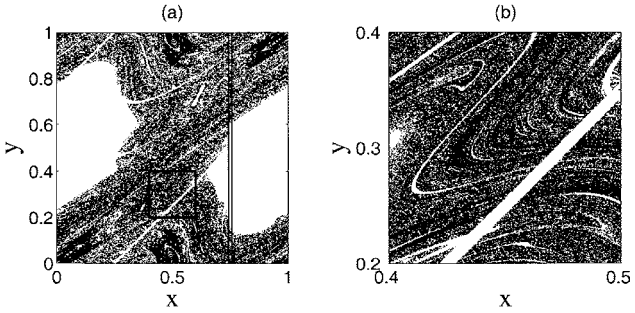

FIG. 4. For $c=0.999$, image of the voltage-protection boundary.

complementary regions Σ_1 and Σ_2, and let the corresponding area-preservating maps be $\mathbf{f}_1(\mathbf{x})$ and $\mathbf{f}_2(\mathbf{x})$, respectively. The regions Σ_1 and Σ_2 are thus the domains of the map functions $\mathbf{f}_1(\mathbf{x})$ and $\mathbf{f}_2(\mathbf{x})$, respectively. In reference to the phase-space structure of a typical Hamiltonian system, we focus on the chaotic sea and analyze the consequence of nonsmoothness on trajectories from the sea. The key observation is the existence of the *forbidden regions* in the phase space caused by the nonsmoothness, which are inaccessible to trajectories under the forward dynamics. In fact, as we will argue, as soon as a parameter changes so that the system becomes nonsmooth, a set of hierarchical regions at all scales appears, trajectories initiated from which must exit it and once exiting, they can no longer return to the set. As a result, a typical trajectory wanders near a chaotic saddle exhibiting transient chaos before approaching one of the final quasiperiodic "attractors."

To see how the forbidden regions arise, consider the inverse maps $\mathbf{x}_n=\mathbf{f}_1^{-1}(\mathbf{x}_{n+1})$ and $\mathbf{x}_n=\mathbf{f}_2^{-1}(\mathbf{x}_{n+1})$. For the exemplary system given by Eqs. (1) and (2), the inverse maps are

$$\begin{aligned} x_n &= x_{n+1} - y_{n+1} - a/b \\ y_n &= y_{n+1} + \sin(2\pi x_n)/b \end{aligned} \quad \text{for } x_n \notin F, \tag{3}$$

and

$$\begin{aligned} x_n &= -x_{n+1} + y_{n+1} + (a+c)/b \\ y_n &= y_{n+1} - 2x_n \end{aligned} \quad \text{for } x_n \in F. \tag{4}$$

Clearly, the dynamics on the set of points that satisfy $\mathbf{f}_1^{(-1)}(\mathbf{P})\in\Sigma_1$ and $\mathbf{f}_2^{(-1)}(\mathbf{P})\in\Sigma_2$ is Hamiltonian so that these points live on invariant sets. Note that, however, for a given point (x_{n+1},y_{n+1}), whether Eq. (3) or Eq. (4) is chosen depends on the value of x_n. Thus, a point (x_{n+1},y_{n+1}) may have two preimages. That is, two points in the phase space can map into one point, which is the origin of dissipationlike properties in the system, despite the Hamiltonian nature of both $\mathbf{f}_1(\mathbf{x})$ and $\mathbf{f}_2(\mathbf{x})$. These points satisfy $\mathbf{f}_1^{(-1)}(\mathbf{P})\in\Sigma_1$ and $\mathbf{f}_2^{(-1)}(\mathbf{P})\in\Sigma_1$ or $\mathbf{f}_1^{(-1)}(\mathbf{P})\in\Sigma_2$ and $\mathbf{f}_2^{(-1)}(\mathbf{P})\in\Sigma_2$. That is, such a point has two preimages and therefore it can go to an "attractor." The remaining set of phase-space points, points that satisfy $\mathbf{f}_1^{(-1)}(\mathbf{P})\in\Sigma_2$ and $\mathbf{f}_2^{(-1)}(\mathbf{P})\in\Sigma_1$, have no preimages and they are forbidden for iterations. Since the forbidden regions lie in the domains of $\mathbf{f}_1(\mathbf{x})$ and $\mathbf{f}_2(\mathbf{x})$, they constitute the basins of attraction of "attractors" in the system.

The key observations are: (1) points in the forbidden regions leave but cannot return to the regions, (2) once trajectories leave they can go to different "attractors," and (3) the forbidden regions are in fact a fat-fractal set [11]. Points in the forbidden regions can then go to different "attractors," no matter how close the points are. This gives rise to the riddledlike structure observed in numerical experiments.

For the voltage-protection circuit system given by Eqs. (1) and (2), the forbidden region $\mathbf{J}$ is the intersecting set between two sets $\mathbf{J}_1$ and $\mathbf{J}_2$ excluding the set of points that go to "attractors," where points in J_1 and J_2 are defined by $x-a/b+m-x_{F_2} \leqslant y \leqslant x-a/b+m-x_{F_1}$ and $x+x_{F_2}-(a+c)/b-m \leqslant y \leqslant x+1-(a+c)/b-m$, respectively, and m is an integer from the modular operation. For $c \lesssim 1$, it can be seen that $\mathbf{J}_1 \in \mathbf{J}_2$ and thus, $\mathbf{J}=\mathbf{J}_1 \cap \mathbf{J}_2=\mathbf{J}_1$. A convenient way to detect the forbidden region numerically is to iterate a boundary of the voltage-protection region F. Figure 4(a) shows 1000 images of 100 points on the boundary at $x=x_{F_1}$ for $c=0.999$, which resembles the chaotic sea in the original Hamiltonian system for $c=1.0$. However, a careful examination of Fig. 4(a) reveals a fractal-like set of blank regions, as shown in Fig. 4(b), the blowup of the region inside the rectangular box in Fig. 4(a). These blank regions are in fact the forbidden regions. It was shown by Mira [12] that chaotic motion in two-dimensional, noninvertible, nonsmooth maps is typically restricted to the images of the boundary at which nonsmoothness in the system equations occurs. The black images in Figs. 4(a) and 4(b) thus point to the existence of a chaotic saddle that gives rise to transient chaos for trajectories approaching the "attractors" in the system.

It is known that chaotic seas in a Hamiltonian system are fat-fractal sets [13]. We have seen that as the system becomes nonsmooth, the chaotic sea becomes basins of attraction due to the appearance of a hierarchy of forbidden regions with positive Lebesgue measure. The boundary set of the forbidden regions consists of the images of phase-space boundaries at which nonsmoothness occurs, which has Lebesgue measure zero. This boundary set is, however, not the basin boundaries. In fact, the forbidden regions contain basins of attractions of all "attractors" in the system and the basin boundaries merely divide the fat-fractal sets on all scales. The numerically obtained near-zero value of the uncertainty exponent indicates that the dimension of the basin boundaries is essentially that of the phase space. The resulted unpredictability of "attractors" is a consequence of the mixing of basins of attraction at all scales on fat fractals. This mechanism for generating riddledlike basins and the total unpredictability of "attractors" is thus characteristically different from those reported previously.

Y.C.L. was supported by AFOSR under Grant No. F49620-03-1-0290. D.R.H. and J.Y.M. were supported by National Natural Science Foundation of China under Grant No. 10275053.

[1] C. Grebogi, S. W. McDonald, E. Ott, and J. A. Yorke, Phys. Lett. **99A**, 415 (1983); S. W. McDonald, C. Grebogi, E. Ott, and J. A. Yorke, Physica D **17**, 125 (1985).

[2] F. T. Arecchi, R. Badii, and A. Politi, Phys. Rev. A **29**, 1006 (1984); F. T. Arecchi and A. Califano, Phys. Lett. **101A**, 443 (1986).

[3] F. C. Moon, Phys. Rev. Lett. **53**, 962 (1984); F. C. Moon and G.-X. Li, *ibid.* **55**, 1439 (1985); E. G. Gwinn and R. M. Westervelt, Phys. Rev. A **33**, 4143 (1986).

[4] J. C. Alexander, J. A. Yorke, Z. You, and I. Kan, Int. J. Bifurcation Chaos Appl. Sci. Eng. **2**, 795 (1992); E. Ott, J. C. Alexander, I. Kan, J. C. Sommerer, and J. A. Yorke, Physica D **76**, 384 (1994); P. Ashwin, J. Buescu, and I. N. Stewart, Phys. Lett. A **193**, 126 (1994); Nonlinearity **9**, 703 (1996); J. F. Heagy, T. L. Carroll, and L. M. Pecora, Phys. Rev. Lett. **73**, 3528 (1994); Y.-C. Lai and C. Grebogi, Phys. Rev. E **52**, R3313 (1995); H. Nakajima and Y. Ueda, Physica D **99**, 35 (1996); L. Billings, J. H. Curry, and E. Phipps, Phys. Rev. Lett. **79**, 1018 (1997); K. Kaneko, *ibid.* **78**, 2736 (1997); Y. L. Maistrenko, V. L. Maistrenko, A. Popovich, and E. Mosekilde, Phys. Rev. E **57**, 2713 (1998); T. Kapitaniak, Y. Maistrenko, A. Stefanski, and J. Brindley, *ibid.* **57**, R6253 (1998); M. Woltering and M. Markus, Phys. Rev. Lett. **84**, 630 (2000).

[5] Y.-C. Lai, C. Grebogi, J. A. Yorke, and S. C. Venkataramani, Phys. Rev. Lett. **77**, 55 (1996).

[6] Y.-C. Lai and R. L. Winslow, Phys. Rev. Lett. **72**, 1640 (1994).

[7] X.-M. Wang, Y.-M. Wang, K. Zhang, W.-X. Wang, H. Chen, Y.-M. Jiang, Y.-Q. Lu, J.-S. Mao, and D.-R. He, Eur. Phys. J. D **19**, 119 (2002).

[8] J. Wang, X.-L. Ding, B. Hu, B.-H. Wang, J.-S. Mao, and D.-R. He, Phys. Rev. E **64**, 026202 (2001).

[9] D.-R. He, B.-H. Wang, M. Bauer, S. Habip, U. Krueger, W. Matienssen, and B. Christiansen, Physica D **79**, 335 (1994).

[10] A. J. Lichtenberg and M. J. Lieberman, *Regular and Stochastic Motion* (Springer-Verlag, New York, 1983).

[11] Y. He, Y.-M. Jiang, Y. Shen, and D.-R. He, Phys. Rev. E **70**, 056213 (2004).

[12] C. Mira, Int. J. Bifurcation Chaos Appl. Sci. Eng. **6**, 895 (1996).

[13] J. D. Farmer, Phys. Rev. Lett. **55**, 351 (1985); D. K. Umberger and J. D. Farmer, *ibid.* **55**, 661 (1985).